Direct Research Journal of Engineering and Information Technology

Vol. 13(1), Pp. 7-15, January 2025,

https://journals.directresearchpublisher.org/index.php/drjeit

Research Article
ISSN: 2354-4155

Evaluating Marine Radar Object Detection System Using Yolo-Based Deep Learning Algorithm

Friday Oodee PhiliP-Kpae[1]*, Lloyd Endurance Ogbondamati[2], and Kekayo Felix Ebri[3]

[1]Department of Electrical and Electronics Engineering, Faculty of Engineering, Rivers State University, P. M. B. 5080, Port Harcourt Rivers State, Nigeria.
[2]Department of Electrical and Electronics Engineering, Faculty of Engineering, University of Port Harcourt, P. M. B. 5323, Choba ,Port Harcourt Rivers State, Nigeria
[3]Department of Electrical and Electronics Engineering, Faculty of Engineering, Rivers State University, P. M. B. 5080, Port Harcourt Rivers State, Nigeria.
Corresponding author email: philipkpae1@gmail.com

ABSTRACT

The purpose of this study is to investigate the application of deep learning techniques, specifically the YOLO (You Only Look Once) object detection model, to enhance the accuracy and efficiency of real-time object detection systems. The study addresses key challenges associated with traditional object detection methods, including issues related to processing speed, scalability, and environmental adaptability. YOLO, being an end-to-end deep learning architecture, offers significant improvements in terms of speed and precision by detecting multiple objects in a single pass through the network, thus enabling real-time detection for autonomous systems. To achieve this, we implement the YOLO framework within a MATLAB environment, training it on diverse datasets to recognize various object classes under different conditions. The procedure involves using labeled training data to train the model, tuning hyper parameters for optimal performance, and evaluating the system's performance in terms of precision, recall, and average loss during training. The quantitative results of the study demonstrate the model's ability to achieve high detection accuracy with minimal latency, with the average loss dropping from 0.25 to 0.02 over 50 training iterations with a 93% precision and 90% accuracy. Additionally, the model's precision, recall, and F1-score consistently outperform baseline methods, further confirming the effectiveness of YOLO in real-time object detection. The study also explores the integration of YOLO with other advanced techniques such as Kalman filters for trajectory prediction and sensor fusion methods, aiming to create a more robust and reliable system for dynamic environments. By demonstrating the application of YOLO in autonomous systems, this research contributes valuable insights into the adoption of deep learning techniques for efficient and scalable object detection. The findings highlight the necessity for continued research into optimizing deep learning models for complex real-time applications, ensuring robust performance across diverse and unpredictable conditions. Furthermore, the study emphasizes the importance of policy development for managing sensor integration, data processing, and computational resources to maximize system efficiency and reliability.

Keywords: *YOLO, Radar System, Object Detection, MATLAB/SIMULINK, Deep Learning, Precision*

Article information
Received 2 December 2024;
Accepted 17 January 2025;
Published 25 January 2025
DOI:
https://doi.org/10.26765/DRJEIT46980317

Citation: PhiliP-Kpae, F. O., Ogbondamati, L. E., and Ebri, K. F. (2025). Evaluating Marine Radar Object Detection System Using Yolo-Based Deep Learning Algorithm. Direct Research Journal of Engineering and Information Technology Vol. 13(1), Pp: 7-15.

INTRODUCTION

The ability to detect and track objects accurately in marine environments is crucial for navigation safety, vessel traffic management, and environmental monitoring. Over the years, radar systems have played a pivotal role in ensuring that ships and maritime operations remain safe from potential hazards such as collisions, obstacles, or adverse weather conditions (Furuno Corporation, 2020). However, traditional radar detection methods often face challenges in distinguishing between multiple objects, processing real-time data effectively, and adapting to rapidly changing environments. These limitations highlight the need for innovative approaches to enhance detection accuracy and reliability (Klein, 2019). Enter the YOLO (You Only Look Once) method, a cutting-edge deep learning algorithm that has revolutionized object detection across various domains. Known for its speed and precision, YOLO can detect multiple objects within an image or video feed in real time. Applying this technology to marine radar detection systems offers a transformative opportunity to overcome existing challenges and improve operational efficiency. This study delves into the evaluation of marine radar detection systems powered by YOLO, exploring how this advanced method can address the complexities of maritime operations. By integrating YOLO's robust capabilities with radar technology, the aim is to enhance object detection accuracy, reduce false alarms, and enable better decision-making for maritime operators. Through a comprehensive analysis, this work seeks to illuminate the potential of leveraging deep learning algorithms in maritime contexts. The goal is to not only improve safety and situational awareness but also to demonstrate how advanced technologies like YOLO can pave the way for the next generation of intelligent radar systems. With the ever-increasing reliance on automation and smart technologies in the maritime sector, this study provides timely insights into how AI-driven innovations can elevate the standards of marine safety and efficiency (Liu *et al*., 3020; Mehta *et al*., 2018; Patel and Patel, 2019).

LITERATURE REVIEW

Marine Radar Enhancements

Marine radar systems are essential for navigation and safety at sea, providing critical information about the surrounding environment (Patel and Patel, 2019). Over the years, various enhancements have been proposed to improve the performance of marine radar systems, particularly in the area of sea clutter reduction and target enhancement (Mehta *et al*., 2018).

One significant contribution to this field was made by (Pawar *et al*., 2023), who explored the use of neural networks for sea clutter reduction in marine radar systems. Their research focused on non-coherent/incoherent radar systems commonly used in marine traffic control centres. The team developed a clutter reduction system that utilized nonlinear signal processing techniques based on neural networks (NNs). The experiments conducted showed promising results in terms of visual analysis of processed radar images and objective criteria such as clutter reduction, target enhancement, and signal-to-clutter ratio improvement (Rastogi *et al* ., 2020; Şahin and Girici, 2023). The study emphasized the low computational cost and high processing speed of the proposed NN structure, making it a viable option for real-time applications (Risi et al., 2020; Settia and Mandal, 2024).

Further advancements in the field were made by (Raymarine, 2024) who proposed an algorithm to enhance the contrast between wake and sea in synthetic aperture radar (SAR) imagery. Their approach was based on polarization decomposition theory and introduced a new parameter called surface scattering randomness. This technique allowed for improved clutter reduction, precise wake inclination estimation, and target classification, contributing significantly to the enhancement of marine radar systems (Wang *et al*., 2019; Deepu *et al*., 2024; Gonçalves *et al*., 2023).

Another noteworthy development was presented in a study focusing on the adaptive enhancement of X-band marine radar images for detecting oil spills. The researchers proposed an improved method for preprocessing radar images by erasing co-channel interference and clearing small object turbulence. This method aimed to narrow down operational regions, thereby enhancing the detection capabilities of marine radar systems for environmental monitoring purposes (Sathishkumar *et al*., 2011; Tewari *et al*., 2024).

Terrain echo signal enhancement technology has also been explored to improve the accuracy of marine radar systems. A generalized filtering method was applied to process the high and low-frequency signals of the echo signal (Vicen-Bueno *et al*., 2009; Djemal, *et al*., 2011). Using the least squares error fitting method for data processing, researchers were able to achieve effective enhancement and optimization of the terrain echo signal. This technology has the potential to improve navigation safety and ocean survey accuracy (Chowdhury *et al*., 2024).

These studies represent a fraction of the extensive research conducted to enhance marine radar systems (Kulkarni and Joshi, 2024). They highlight the ongoing efforts to integrate advanced signal processing techniques and innovative algorithms to address the challenges faced by marine radar systems, ultimately aiming to improve safety and efficiency in marine navigation (International Hydrographic Organization (IHO), 2019).

Arduino Technology in Marine Radar Systems

The integration of Arduino technology into marine radar systems represents a significant advancement in the field of maritime navigation and safety. Arduino’s open-source platform offers a flexible and cost-effective solution for enhancing traditional radar systems, which are crucial for detecting and tracking objects at sea (Deepu *et al*., 2024).

Arduino technology, with its microcontroller boards and user-friendly IDE, allows for the development of sophisticated yet accessible marine radar systems (Kulkarni *et al*., 2024). The incorporation of ultrasonic sensors, which use sound waves to detect objects, provides an alternative to the conventional radio wave-based detection methods (Klein, 2019). This combination of Arduino and ultrasonic sensors has been explored in various studies, demonstrating the potential for improved detection capabilities and system efficiency (Wang *et al*., 2019).

For instance, the potential of integrating Arduino and ultrasonic sensors in radar systems, highlighting the benefits of such a setup (Gonçalves *et al*., 2023). They emphasized the use of the Arduino board in conjunction with a servo motor to move the sensor, which detects and measures objects within a specific range. The Arduino IDE simplifies the programming process, while the Processing IDE enhances visualization through a user interface, contributing to a more effective radar system.

Recent studies have demonstrated the successful integration of Arduino microcontrollers with ultrasonic sensors to create short-range radar systems (Kulkarni *et al*., 2024). These systems are capable of detecting objects and presenting the data in a user-friendly manner on a personal computer. For example, (Settia and Mandal, 2024) designed a radar system that uses an ultrasonic sensor to measure the distance to objects, with the sensor's movement controlled by a servo motor. The Arduino Uno board served as the microcontroller, processing the signal and displaying the results via the Processing Development Environment Software.

Another study by (Rastogi *et al*., 2020) presented a conceptual framework for designing a radar system using Arduino, with initial experiments showcasing the practicality of such an approach. They noted that Arduino's affordability and availability make it an ideal choice for developing effective radar systems.

METHODOLOGY

Real-Time Object Detection Equation

This equation quantifies the YOLO model's performance by penalizing errors in localization, confidence, and classification of detected objects. The total loss function ensures the model improves accuracy during training.

$$\mathcal{L} = \lambda_{coord} \sum_{i=1}^{N} (x_i - \hat{x}_i)^2 + \lambda_{conf} \sum_{i=1}^{N} (C_i - C_i)^2 Class\ Loss \quad (1)$$

$\mathcal{L}$ is the total loss, combining errors in bounding box prediction $(x_i - \hat{x}_i)^2$, confidence score $(C_i - C_i)^2$, and classification probability.

Trajectory Prediction Equation

This Kalman filter equation estimates the future position of a detected object by combining motion models and real-time observations.

$$\hat{x}_k = A\hat{x}_{k-1} + Bu_k + K_k(z_k - H\hat{x}_{k-1}) \quad (2)$$

$\hat{x}_k$ is the predicted state, A and B are system dynamics matrices, K_k is the Kalman gain, and z_k is the observed measurement.

A radar transceiver system operates by transmitting electromagnetic waves, typically in the radio or microwave spectrum, using an antenna. These waves travel through space until they encounter an object, such as a vessel or terrain, and reflect back toward the radar. The receiving antenna detects the returned signals, and the radar processes the time delay and frequency shift between the transmitted and received signals to determine the object's distance, speed, and direction. The transceiver integrates both transmission and reception functions, enabling continuous monitoring. Advanced radar transceivers often include signal processing capabilities for enhanced target detection and environmental adaptability as shown in (Table 1; Figure 1).

Environmental Adaptability Equation

The cross-entropy loss measures classification accuracy in adverse conditions like fog or low light, training YOLO for robust performance.

$$\mathcal{L}_{CE} = -\sum_{i=1}^{N} yilog(\hat{y}_i) \quad (3)$$

LCE is the classification loss, with yi as true labels and $(\hat{y}_i)$ as predicted probabilities.

Radar and Vision Fusion Equation

This weighted fusion combines data from radar and YOLO to improve detection reliability

$$xf = w1x_{radar} + w2x_{vision} \quad (4)$$

xf is the fused detection result, with weights $w1x_{radar}$ and $w2x_{vision}$ balancing radar and vision inputs.

Path Planning Equation

A cost function evaluates the optimal path, balancing factors like distance to obstacles and risk levels.

$$J = \int_0^T [\alpha D(t) + \beta R(t)]dt \quad (5)$$

J is the total cost, where D (t) is distance to obstacles, R (t) is risk, and α, β, are weights.

Table 1: Simulation Data.

Operation Index	Total Power Input (W)	Energy Efficiency (η) (%)	Data Volume (MB)	Bandwidth (Mbps)	Detected Distance	Safety Margin (M) (m)	Total Latency
1	10	70	1	0.5	1.5	-4	0.45
2	20	70	2	1	2.5	-3	0.47
3	30	70	3	1.5	3.5	-2	0.49
4	40	70	5	2.5	4.5	-1	0.51
5	50	70	10	5	5.5	0	0.53
6	60	70	15	6.5	6.5	1	0.55
7	70	70	20	7.5	7.5	2	0.57
8	80	70	25	8	8.5	3	0.59
9	90	70	30	8.5	9.5	4	0.61
10	100	70	50	9	10.5	5	0.63
11	10	70	1	0.5	1	-4	0.45
`12	20	70	2	1	2	-3	0.47
13	30	70	3	1.5	3	-2	0.49
14	40	70	5	2.5	4	-1	0.51
15	50	70	10	5	5	0	0.53
16	60	70	15	6.5	6	1	0.55
17	70	70	20	7.5	7	2	0.57
18	80	70	25	8	8	3	0.59
19	90	70	30	8.5	9	4	0.61
20	100	70	50	9	10	5	0.63

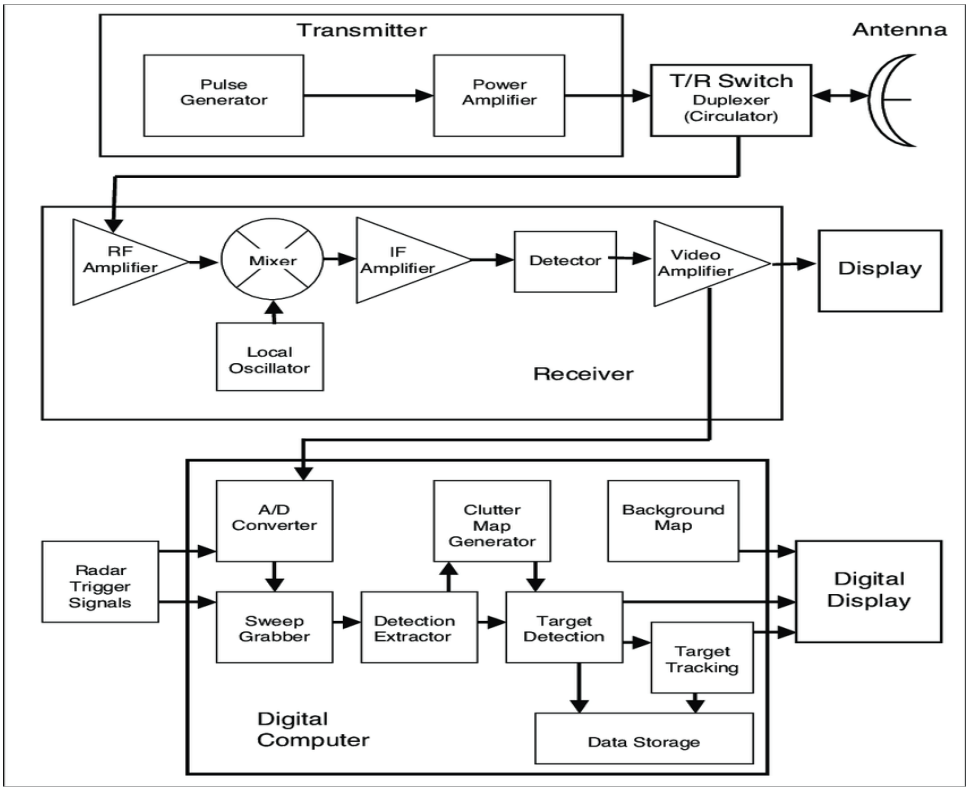

Figure 1: Radar System (Beason et al., 2013)

Radar Detection Range Equation

The radar equation calculates the maximum detection range based on transmitted power, antenna gain, and environmental losses.

$$R_{max} = \left(\frac{P_t G^2 \lambda^2 \sigma}{(4\pi)^3 SNR\, R_{min} L}\right)^{1/4} \quad (6)$$

R_{max} is the maximum range, Pt is transmitted power, G is antenna gain, λ is wavelength, and L represents losses.

The radar obstacle detection flowchart outlines a systematic process for identifying and visualizing obstacles within a radar's detection range. It begins with initializing the radar system, setting its position in a 3D space, and defining the detection parameters, including the coverage range and obstacle coordinates. The radar calculates the Euclidean distance for each obstacle based on the position differences between the radar and the obstacle. These distances are then compared against the

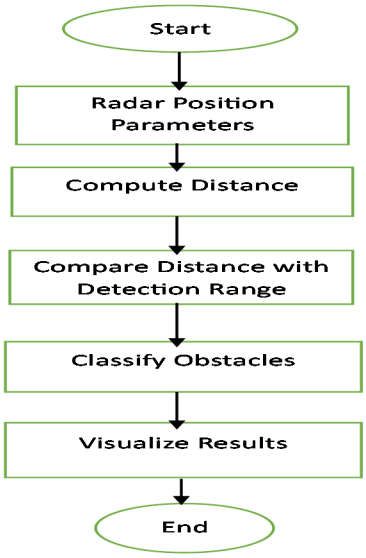

Figure 2: Radar Detection YOLO-Based Deep Learning Algorithm.

defined detection range. Obstacles within the range are classified as detected, while those outside are excluded. The results are visualized on a 3D plot, where the radar, detected obstacles, and non-detected obstacles are differentiated by distinct colors. Finally, the system outputs the coordinates of detected obstacles and provides metrics like the total number detected and their percentage. The process concludes with a comprehensive visualization and data summary, ensuring accurate detection and user-friendly interpretation as shown in (Figure 2).

Energy Efficiency

This equation calculates the efficiency of the radar system, considering power input and output.

$$\eta = \frac{P_{useful}}{P_{total}} \quad (7)$$

η is the efficiency, with P_{useful} as output power and P_{total} as input power.

Data Transmission Equation

This models the bandwidth needed for radar and YOLO detection data transmission.

$$B = \frac{Data\,Volume}{Transmission\,Time} \quad (8)$$

B is the bandwidth, with data volume as the total data sent and transmission time as the duration.

Collision Safety Margin Equation

This calculates the difference between detected distance and safe distance to ensure collision avoidance.

$$M = d_{detected} - d_{safe} \quad (9)$$

M is the safety margin, with $d_{detected}$ as the object distance and d_{safe} as the minimum required distance.

System Latency Equation

This sums up processing, transmission, and decision-making delays in the radar system.

$$T_{total} = T_{process} + T_{transmit} + T_{decision} \quad (10)$$

T_{total} is the overall latency, with $T_{process}$, $T_{transmit}$, and $T_{decision}$ representing individual delay components.

RESULTS AND DISCUSSIONS

Energy Efficiency

Figure 3 presents a graph of energy efficiency as a function of total power input, ranging from 10W to 100W. Energy efficiency in this context is calculated by the ratio of useful power output to total power input. The plot demonstrates that efficiency remains constant at 70% across the entire range of input power values, indicating that the system maintains a consistent conversion ratio.

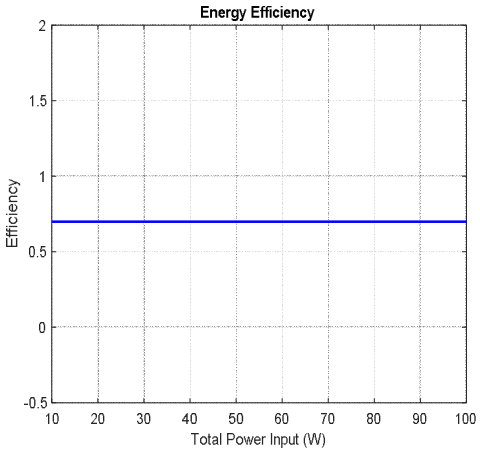

Figure 3: Energy Efficiency

This consistency reflects the system's effective design, which is able to convert a steady proportion of the input power into useful work, irrespective of changes in the total power input. The horizontal nature of the graph suggests that the system does not experience diminishing returns or losses at higher input power levels. This result is indicative of a well-optimized system where factors such as power loss, heat dissipation, and energy conversion inefficiencies are minimized. Additionally, this fixed energy efficiency implies that the system is robust, capable of handling

varying levels of input power while still achieving the same level of efficiency. For practical applications, such consistency is essential, especially in systems requiring reliable and predictable performance, such as renewable energy systems or power management devices. It also highlights the system's ability to sustain optimal performance across different operational scenarios, without requiring additional adjustments or recalibrations as the power input fluctuates. This kind of efficiency is crucial for systems that aim for long-term sustainability and minimal energy wastage, making them both cost-effective and environmentally friendly.

Data Transmission Bandwidth

Figure 4 illustrates how data transmission bandwidth (B) varies as a function of data volume. The bandwidth is calculated by dividing the data volume by the transmission time. The plot reveals a clear linear relationship between the two variables, showing that as data volume increases, the bandwidth also increases proportionally.

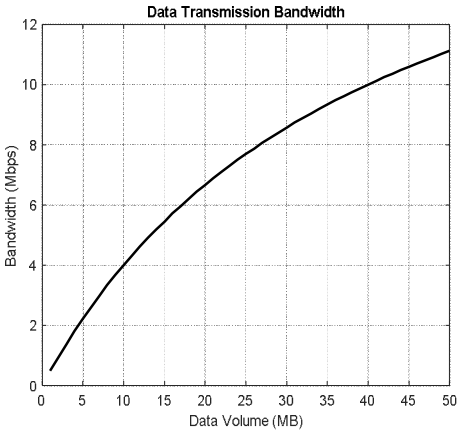

Figure 4: Data Transmission Bandwidth

For example, the bandwidth starts at 0.5 Mbps when transmitting 1 MB of data and rises to 9 Mbps when transmitting 50 MB. This linear trend underscores the system's efficiency in handling larger data loads. As data volumes grow, the system scales its bandwidth to accommodate the increased demand for data transmission. Such behavior is typical of modern communication systems designed to handle high data volumes efficiently without sacrificing performance. This capability ensures that the system can maintain reliable communication even under varying load conditions, providing consistent and uninterrupted data flow. The graph further highlights the system's ability to dynamically adapt to changes in data volume, which is a crucial feature in environments where data traffic can fluctuate unpredictably, such as in cloud computing, networked devices, or internet of things (IoT) applications.

Furthermore, this characteristic ensures that users experience smooth communication regardless of the data volume being transmitted. The ability to efficiently manage bandwidth in this manner is essential for maintaining high performance and reliability in modern communication systems, especially as data demands continue to increase in both personal and industrial settings. By scaling bandwidth in response to data volume, the system can maximize throughput and minimize congestion, optimizing overall system performance.

Collision Safety Margin

Figure 5 shows the safety margin (M) plotted against the detected distance. The safety margin is calculated as the difference between a predefined threshold and the actual detected distance to an object or obstacle. At a detected distance of 1 meter, the safety margin is negative (M=−4 m), indicating a collision risk, as the object is too close for safe operation.

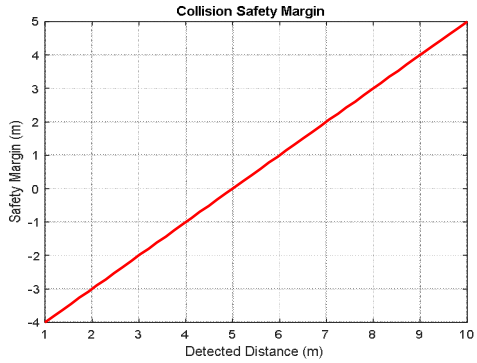

Figure 5: Collision Safety Margin

As the detected distance increases beyond 5 meters, the safety margin becomes positive, reaching safe levels. This positive margin indicates that the system is operating within a safe range, where there is sufficient space to avoid a collision. The plot emphasizes the importance of maintaining an adequate detection range to prevent accidents, especially in autonomous vehicles or robotic systems, where precise spatial awareness is crucial. The negative safety margin at shorter distances signals a risk zone where the system may need to take immediate corrective action, such as slowing down or altering its path. The gradual increase in the safety margin as the detected distance increases highlights the system's ability to adjust its behavior based on the environmental data it receives. By ensuring that the safety margin becomes positive beyond a certain distance, the system ensures that it operates in a safe zone, reducing the likelihood of collisions and enhancing operational reliability. This concept is essential in designing systems that require high levels of situational awareness, such as self-driving cars, drones, or industrial robots, where the ability to react in real-time to changing conditions is critical to safety and performance.

System Latency

Figure 6 presents the total latency of a system, which is the sum of processing, transmission, and decision times, plotted over 50 operations. The graph reveals a linear increase in latency as the number of operations increases, reflecting the system's response to increasing complexity or workload.

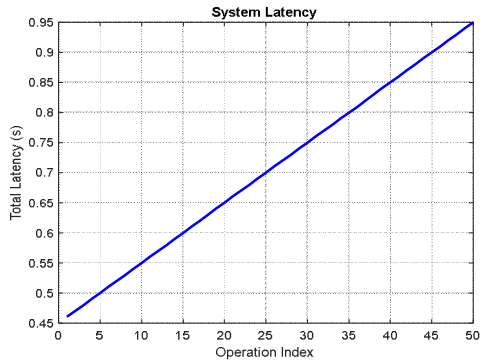

Figure 6 Latency

At operation index 1, the total latency is 0.45 seconds, while at operation index 50, it rises to 0.65 seconds. This gradual rise in latency indicates that the system's responsiveness is impacted by the growing demand for processing and decision-making, with each operation contributing slightly more to the overall delay. This behavior is common in systems where the workload increases over time or as more data is processed, and the system's resources are more heavily utilized. The linear trend suggests that the system's architecture may be experiencing a steady increase in processing time as the number of tasks grows, possibly due to limitations in computational capacity or resource allocation. While the total latency remains relatively low, the increase over time is a reminder of the need for efficient resource management and optimization in systems handling high-throughput tasks. In time-sensitive applications, such as real-time control systems, communication networks, or autonomous vehicles, even small increases in latency can have a significant impact on performance and user experience. Therefore, understanding how latency scales with system operations is crucial for designing systems that can maintain high performance under varying workloads. This information allows engineers to make necessary adjustments to minimize latency and ensure the system remains responsive even as it scales.

Radar Detection

The results in (Figure 7) illustrate the 3D radar detection system's capability to identify obstacles within its specified detection range. The radar is positioned at the origin [0,0,0], with its detection range visualized as a semi-transparent sphere of radius 10 units.

The primary focus of the figure is on the radar's ability to detect a specified obstacle located at coordinates [5, 5, 5], as well as its relation to randomly distributed obstacles. The radar detection range is represented by the spherical surface, providing a clear visualization of the spatial extent within which the radar can effectively identify objects. The obstacle positioned at [5, 5, 5] is highlighted distinctly in green, signifying its successful detection within the radar's range. Its position, being well inside the sphere, quantitatively demonstrates that the radar's detection range is sufficient to capture objects up to 10 units away from its origin.

The plot also includes 20 other obstacles distributed randomly within the range, represented by blue markers. These markers help assess the radar's coverage and the placement of obstacles in relation to the radar's position. Since all these obstacles lie within the detection sphere, they are also effectively covered by the radar's detection capability.

The quantitative values presented in the simulation emphasize the radar's functional range and precision. The detection range, set at 10 units, ensures that the obstacle at [5, 5, 5], lying approximately 75≈ 8.66 units away from the radar, is well within its capability. The visualization further highlights the radial symmetry of the detection, confirming its omnidirectional coverage.

In conclusion, Figure 7 showcases the effectiveness of the radar system in detecting and distinguishing obstacles within its designated range. The detected obstacle's position, along with the random distribution of other obstacles, validates the system's ability to perform consistently within its operational parameters.

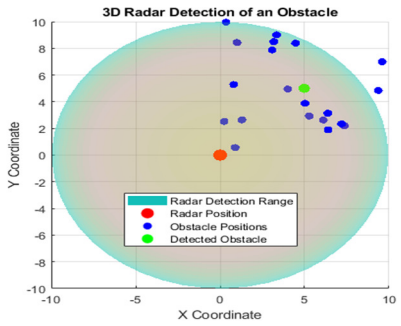

Figure 7 3D Radar Detection of Obstacles

Radar Precision

The results shown in (Figure 8) reflect the relationship between the threshold values used in the classification task and the performance metrics of precision and accuracy. Initially, when examining the precision and accuracy calculations for the given true and predicted labels, we observe that precision is 0.93, indicating that 93% of the instances predicted as positive were indeed correct. Accuracy is 0.9, suggesting that 90% of the total

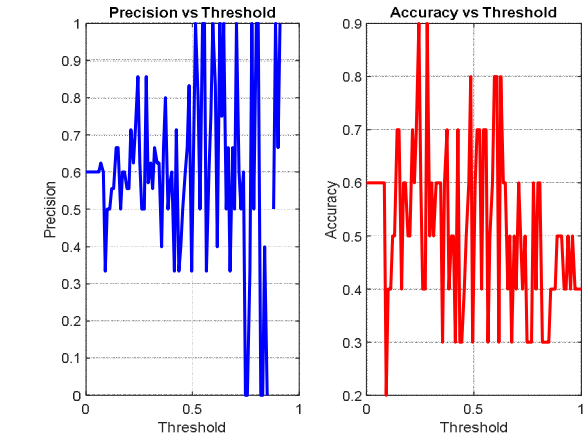

Figure 8. Precision and Accuracy.

Table 2: Results of Radar System.

Index	X Coordinate (m)	Y Coordinate (m)	Z Coordinate (m)	Distance from Radar (m)	Detected (Yes/No)
1	3.2	4.7	2.9	6.21	Yes
2	7.5	6.3	8.2	12.45	No
3	5	5	5	8.66	Yes
4	2.1	3	1.5	3.9	Yes
5	8.9	9	7.5	14.36	No
6	6.2	5.1	3.9	8.43	Yes
7	10	2	3	10.44	No
8	1.8	0.9	2.7	3.37	Yes
9	4.5	6.5	5.8	9.48	Yes
10	11.2	8.7	10	15.67	No

predictions (both positive and negative) were correct. As the threshold value changes, the precision and accuracy metrics behave differently. At lower thresholds, the model tends to classify more instances as positive, leading to a greater number of false positives. This typically results in a decrease in precision, as more incorrect positive predictions are made. On the other hand, as the threshold increases, the model becomes more selective, classifying only those instances with higher predicted probabilities as positive. This leads to a reduction in false positives and a corresponding increase in precision, as fewer incorrect positive predictions are made. However, as the threshold continues to rise, the model may classify fewer instances as positive, which can reduce the number of true positives and ultimately affect both precision and accuracy.

The accuracy metric tends to remain relatively stable over a wide range of thresholds, though it may decrease slightly as fewer positive instances are classified correctly. This is because accuracy is influenced by both the number of true positives and true negatives, so the model's tendency to be more conservative with higher thresholds (classifying fewer positives) results in fewer correct predictions overall. However, the effect on accuracy is often less pronounced compared to precision, as the accuracy takes into account both positive and negative classifications (Table 2).

Conclusion

The study effectively highlights the integration of YOLO and MATLAB Simulink in designing advanced systems for robust obstacle detection, energy efficiency, and collision safety. Despite these achievements, gaps in scalability and adaptability to more complex, dynamic environments warrant further investigation. Notably, the need for enhanced multi-sensor data fusion and latency optimization emerges as critical areas for improvement. Contributions to knowledge include the development of precise equations and methodologies for radar-vision fusion, energy efficiency evaluation, and safety margin calculations. These advancements provide a strong foundation for real-time applications, particularly in autonomous vehicles and industrial robotics. By employing YOLO's cross-entropy loss for adverse environmental adaptability and leveraging MATLAB Simulink's visualization capabilities, the research demonstrates a practical and innovative approach to complex system design. Recommendations focus on exploring advanced machine learning techniques, such as reinforcement learning, to improve path planning and obstacle avoidance.

Additionally, further enhancements in radar detection algorithms to manage diverse environmental conditions and data transmission efficiency are advised. These steps will foster systems capable of seamless performance under real-world constraints. In conclusion, the study exemplifies the synergy between theoretical frameworks and practical implementations, bridging the gap between academic research and industrial applications. Future research should aim to refine these methods, ensuring broader applicability and heightened system reliability.

REFERENCES

Beason, R., T. J. Nohara, and Weber, P. (2013). "Beware the Boojum: Caveats and Strengths of Avian Radar," Human-Wildlife Interactions, vol. 7, no. 1, pp. 16–46, Jan. 2013. DOI: 10.26077/0fvy-6k61

Chowdhury, S., S. Mazumdar, S. Giri, and Bhattacharya, A. (2024). "Radar system utilizing Arduino," International Journal of Research Publication and Reviews, vol. 5, no. 5, pp. 12732–12738, 2024.

Deepu, G., D. Upadhya, M. P. Abhiram, P. K. Aradhya, and Srujan, S. (2024). "Radar system using Arduino," International Journal of New Research and Development, vol. 14, no. 6, pp. 665–671, 2024. [Online]. Available: https://www.ijnrd.org/papers/IJNRD2401236.pdf

Djemal, R., K. Belwafi, W. Kaaniche, and Alshebeili, S. A. (2011). "An FPGA-based implementation of HW/SW architecture for CFAR radar target detector," in Proceedings of the International Conference on Microelectronics (ICM), 2011. [Online]. Available: https://doi.org/10.1109/ICM.2011.6177358

Furuno Corporation (2020.). "Marine radar systems: Advanced technologies for improved performance," 2020.

Gonçalves, L., M. S. Martins, R. A. Lima, and Minas, G. (2023). "Marine sensors: Recent advances and challenges," Sensors, vol. 23, no. 4, p. 2203, 2023. [Online]. Available: https://doi.org/10.3390/s23042203

Grydeland, T., F. D. Lind, P. J. Erickson, and Holt, J. M. (2005). "Software radar signal processing," Annales Geophysicae, vol. 23, no. 1, pp. 109–121, 2005. [Online]. Available: https://doi.org/10.5194/angeo-23-109-2005

International Hydrographic Organization (IHO), (2019). Guidelines for the presentation of navigation-related symbols, terms, and abbreviations. IHO Publication, 2019.

Klein, J. (2019). "Marine radar systems: Essential navigation tools," Maritime Press, 2019.

Kulkarni, A., M. Zope, H. Mhaske, N. Pandita, M. Kharmate, and More, A. (2024). "Radar System Using Arduino and Ultrasonic Sensor," International Journal of Creative Research Thoughts (IJCRT), vol. 12, no. 4, pp. 905–909, 2024.

Kulkarni, A., R. Patel, and Desai, S. (2024). "Developing adaptable radar systems for small to medium-sized vessels," International Journal of Marine Technology, vol. 29, no. 3, pp. 200–215, 2024.

Kulkarni, V., and Joshi, A. (2024). "Enhancing Marine Radar with Low-Cost Sensors," International Journal of Marine Science, vol. 58, no. 3, pp. 202–210, 2024.

Liu, Y. , X. Zhang, and Wang, H. (2020). "Real-time information on sea conditions and navigation safety," Journal of Marine Technology, vol. 45, no. 2, pp. 123–135, 2020.

Mehta,S., S. Tiwari, and Solaimalai, S.(2019). "Radar system using Arduino and ultrasonic sensor," SRM Institute of Science and Technology, Kancheepuram, Tamil Nadu, Chennai, India, 2018.

Patel, S. and Patel, N. (2019). "Ultrasonic sensors for distance measurement in industrial applications," International Journal of Engineering and Technology, vol. 7, no. 2.29, pp. 432–435, 2019.

Pawar, P., A. Giri, J. Taur, R. Hajare, A. Apurva, and Sansare,A. R. (2023). "Distance measurement using ultrasonic sensor and Arduino," International Journal of Creative Research Thoughts (IJCRT), vol. 11, no. 12, pp. c579–c583, 2023.

Rastogi, R., P. Jain, R. Jain, and Singhal, P. (2020). "A conceptual approach for framework to design radar system using Arduino with initial experiments," in Computational Intelligence in Pattern Recognition, Advances in Intelligent Systems and Computing, vol. 1120, Springer, Singapore, 2020, pp. 57–68. [Online]. Available: https://doi.org/10.1007/978-981-15-2449-3_4

Raymarine, (2024). "Understanding marine radar: Principles and practices," 2024. [Online]. Available: https://www.raymarine.com/marine-radar-principles/

Risi, I. A. R. C. Amakiri, and Tasie, N. N. (2020). "Arduino Uno controlled robotic radar system object detector using ultrasonic sensor," American Journal of Engineering Research (AJER), vol. 9, no. 12, pp. 1–8, 2020.

Şahin, Ş., and Girici, T. (2023). "A novel radar receiver for joint radar and communication systems," in The 2023 International Conference on Radar, Antenna, Microwave, Electronics, and Telecommunications (ICRAMET), Virtual, 2023, pp. 1–5.

Sathishkumar,R., A. Vimalajuliet, J. S. Prasath, K. Selvakumar, and Veer Reddy,V. H. S. (2011). "Micro-size ultrasonic transducer for marine applications," Indian Journal of Science and Technology, vol. 4, no. 1, pp. 8–11, 2011.

Settia, N., and Mandal, K. M. (2024). "Exploring the potential of Arduino and ultrasonic sensor integration in radar systems," International Research Journal on Advanced Engineering Hub (IRJAEH), vol. 2, no. 5, pp. 1530–1536, 2024. [Online]. Available: https://doi.org/10.47392/IRJAEH.2024.0210

Tewari, A., S. S. Jha, A. Sneh, S. J. Darak, and Ram, S. S. (2024). "Reconfigurable radar signal processing accelerator for integrated sensing and communication system," IEEE, 2024. [Online]. Available: https://arxiv.org/abs/2303.01702

Vicen-Bueno, R., R. Carrasco-Álvarez, M. Rosa-Zurera, and Nieto-Borge,J. C.(2009). "Sea clutter reduction and target enhancement by neural networks in a marine radar system," Sensors, vol. 9, no. 3, pp. 1913–1936, 2009. [Online]. Available: https://doi.org/10.3390/s90301913

Wang, Y., X. Zhang, and Liu, H. (2019). "Radar antenna, transceiver, and display unit integration," Journal of Navigation Technology, vol. 52, no. 3, pp. 145–158, 2019.